Microcalorimetric, FTIR, and DFT studies of the adsorption of isobutene on silica

M.A. Natal-Santiago, J.J. de Pablo and J.A. Dumesic*

Department of Chemical Engineering, University of Wisconsin, Madison, WI 53706, USA

Received 16 April 1997; accepted 2 July 1997

Microcalorimetric measurements, infrared spectroscopic studies (FTIR), and quantum-chemical calculations based on density-functional theory (DFT) were made of the interactions of isobutene with silica at 300 K. On the basis of DFT calculations and FTIR spectra, most of isobutene adsorbs reversibly on silica at 300 K, involving the interaction of the π-bond with hydroxyl groups on the surface. The average energy of these interactions is ~45 kJ/mol at a surface coverage of ~400 μmol of isobutene per gram of silica. The formation of butoxy and 2-methyl-1-propoxy species upon reaction of isobutene with silanol groups appears to be limited kinetically at 300 K. While the enthalpies of formation of these species from gaseous isobutene and silanol groups are calculated to be −55 and −40 kJ/mol, respectively, the activation energies for the formation of these species from adsorbed isobutene are estimated from DFT to be 172 and 226 kJ/mol, respectively. These high activation barriers are caused by the required localization of positive charge in the corresponding transition states, which is made difficult by the weak acidity of silica. Minor amounts of surface butoxy might form on silica at 300 K, perhaps on defect or impurity sites, and these species may be responsible for the higher heats of adsorption (56 ± 2 kJ/mol) measured at low surface coverages on silica.

Keywords: isobutene, silica, adsorption, alkoxy, butoxy, microcalorimetry, density-functional theory (DFT), Fourier-transform infrared spectroscopy (FTIR)

1. Introduction

Reactions of light alkenes over solid acid catalysts are of importance in industrial processes such as hydrocarbon cracking, alkylation, and isomerization [1]. An alkene of particular importance is isobutene, which is an intermediate in the production of *t*-butyl alcohol, methyl *t*-butyl ether, and other blending compounds for unleaded gasoline [2]. In addition, isobutene is employed in alkylation processes to produce branched hydrocarbons used in reformulated gasoline [2]. The reactivity of light alkenes over solid acids generally depends on the acid strength of the catalyst [1,3,4]. Moreover, the nature of the hydrocarbon fragments that result from the adsorption of light alkenes on inorganic oxides depends on the acidity of the catalyst surface. These adsorbed species have been proposed to resemble alkoxy complexes on the surface of moderately to strongly acidic oxides such as zeolites [1]. However, the factors that control the formation of these alkoxy species in relation to the acidity of the catalyst are not yet understood in quantitative detail.

In the present study, we report results from studies of isobutene adsorption on silica. We have chosen initially to study silica, since this oxide is generally considered to be a weak acid. Thus, we will address the origin of the low reactivity of this weakly acidic oxide with an alkene such as isobutene. Our approach is (1) to use heat-flow microcalorimetry to measure the heats of interaction of isobutene with silica, (2) to employ Fourier-transform infrared spectroscopy (FTIR) to determine the nature of the surface species formed from isobutene on silica, and (3) to perform quantum-chemical calculations on the basis of density-functional theory (DFT) to probe the potential energy surface (PES) involved in the activation of isobutene on silica. We will show that the transformation of weakly adsorbed isobutene to more strongly adsorbed isobutoxy species is a highly activated process on a weak solid acid such as silica. In addition, the 1,2-hydride shift involved in the transformation between isobutoxy and 2-methyl-1-propoxy species is highly activated over silica.

* To whom correspondence should be addressed.

2. Methodology

2.1. Microcalorimetric measurements

Microcalorimetric measurements were performed at 300 K by using a Tian–Calvet heat-flow microcalorimeter (Seteram C80) connected to a calibrated dosing system, which is equipped with a capacitance manometer (Baratron, MKS Instruments) to measure the pressure of the probe molecule over the sample. A detailed description of the apparatus can be found elsewhere [5,6]. Prior to each experiment, approximately 500 mg of Cab-O-Sil (~380 m^2/g) was outgassed for 2 h at 473 K and subsequently cooled to room temperature.

Afterwards, the microcalorimetric cells were placed in the thermal block, and measurements were initiated after the cells had equilibrated with the calorimeter at 300 K (typically overnight). Isobutene (Matheson, 99.5%) was purified by performing freeze–pump–thaw cycles.

2.2. FTIR measurements

Infrared spectra were collected at room temperature with a resolution of 2 cm^{-1} using a Mattson Galaxy 5020, FTIR spectrometer. Cab-O-Sil was pressed into a self-supporting pellet of $\sim$12 mm in diameter at a pressure of $\sim$70 MPa. Prior to measurements, the sample was outgassed at $\sim$473 K for 1 h under vacuum ($\sim$1 mPa) inside a cell equipped with CaF_2 windows. After collecting the spectrum for silica, isobutene was admitted into the cell at a pressure of 3 kPa, and spectra for isobutene on silica and in the gas phase were collected. Finally, the sample was outgassed overnight at room temperature, and a spectrum was collected for silica after exposure to isobutene.

2.3. DFT calculations

Quantum-chemical calculations were performed on the basis of density-functional theory (DFT), using the three-parameter functional B3LYP [7] along with the basis set 6-31+G* [8]. Detailed information about the theory can be found elsewhere [9,10]. The DFT calculations were performed using the software package GAUSSIAN 94® [11] on an IBM SP2 computer. Structural parameters for isobutene, a silanol group, and the species resulting from their interactions were determined by optimizing to stationary points on the PES corresponding to the stoichiometries C_4H_8, H_3SiOH, and C_4H_8-$HOSiH_3$, respectively, using the Berny algorithm and redundant internal coordinates [12]. A hydrogen-terminated silanol group (H_3SiOH) was chosen to model the surface of silica in order to minimize computational efforts. To refine these computations, one can terminate the cluster with hydroxyl groups instead of hydrogen atoms, add one or more units of silicon, and/or increase the size of the basis set used.

Transition states were located according to a STQN method, which uses a linear or quadratic synchronous transit approach to get closer than an initial guess to the quadratic region of the PES, followed by a quasi-Newton or eigenvector-following algorithm to complete the optimization [13]. These optimizations were also performed using redundant internal coordinates. Optimization criteria consisted of maximum forces and displacements of less than 22 J/(mol pm) and 0.10 pm, respectively, in addition to root-mean-squared forces and displacements of less than 15 J/(mol pm) and 0.06 pm. The resulting molecular structures were classified as local minima or transition states on the PES by calculating the Hessian (force-constants) matrix analytically. For local minima, all eigenvalues of the Hessian matrix were positive, whereas for transition states only one eigenvalue was negative [14]. The vibrational frequencies obtained from the analysis of force constants were used further without scaling, unless specified otherwise, to estimate the thermochemical properties of the clusters of interest at 298 K. To verify that the transition states correspond to the chemical reactions of interest, intrinsic reaction coordinate (IRC) calculations were performed using mass-weighted internal coordinates to follow the reaction path [15,16], that is, the reaction coordinate is expressed in units of length$\cdot\sqrt{\text{mass}}$ [17]. Finally, the optimized molecular structures discussed in the text are defined in terms of cartesian coordinates in the appendix to facilitate their visualization with any suitable software package.

3. Results and discussion

3.1. Microcalorimetric measurements

Microcalorimetric data for the adsorption of isobutene on silica at 300 K are shown in figure 1 in the form of differential heat of adsorption versus isobutene coverage. For convenience, the differential heat of adsorption has been defined as the negative of the differential change in enthalpy for the adsorption process. The adsorption isotherm is included in figure 2. The initial heat of isobutene adsorption on silica is 56 ± 2 kJ/mol, which is slightly higher than the isosteric heat of adsorption of 38 kJ/mol obtained from independent studies [18]. As the coverage of isobutene increases, the heat of adsorption decreases monotonically, because of the energetic heterogeneity of the surface or possibly because of lateral interactions between adsorbed species.

The adsorption of isobutene on silica at temperatures below 220 K has been suggested to involve mainly the interaction of the π-bond with hydroxyl groups on the surface of silica [19,20]. However, at higher temperatures, it is possible for isobutene to react further with the surface to form butoxy species, as explored further in the next two sections by combining quantum-chemical calculations with FTIR spectra.

3.2. DFT calculations

To study the adsorption and reaction of isobutene on silica, three clusters were used that involve a hydrocarbon fragment (C_4H_8) interacting with a hydrogen-terminated silanol group (H_3SiOH). These three clusters represent (1) molecular adsorption involving interactions of the π-bond of isobutene with the hydroxyl group, (2) protonation of a terminal carbon to form isobutoxy species, and (3) protonation of the central carbon

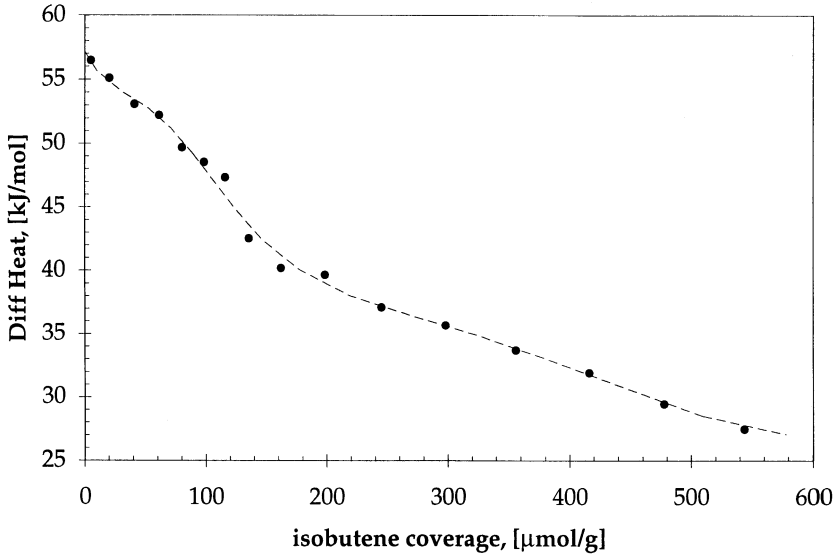

Figure 1. Differential heat versus surface coverage for the adsorption of isobutene on silica at 300 K. The dotted curve (trend) was obtained from a polynomial fit of the integral heat curve.

to form 2-methyl-1-propoxy species. In addition, transition states for the transformation of molecularly-adsorbed isobutene into the two alkoxy species were located in the PES to estimate the rates of these elementary reactions.

The optimized structure for molecularly-adsorbed isobutene is shown in figure 3. In this mode of adsorption, the carbon skeleton is predicted to remain coplanar, with little perturbation of the C=C bond; adsorbed isobutene is predicted to retain a local C_{2v} symmetry. Similarly, the O–H bond in the silanol group is predicted to be perturbed slightly, resulting in a stretch of 1 pm. These perturbations are noticeable if one follows the position of IR bands in the absorption spectra corresponding to the stretching modes of the C=C and O–H bonds. According to our calculations, shifts to lower wavenumbers of 14 and 160 cm^{-1} are predicted for the stretching frequencies of these bonds, respectively. Moreover, a rather low enthalpy change of −10 kJ/mol is predicted for the adsorption of isobutene on silica, which supports the weak nature of the interactions (table 1).

The optimized structures for isobutoxy and 2-methyl-1-propoxy species on silica are shown in figure 4. Energetics obtained from our calculations are summarized in table 1. In these cases, cleavage of the C=C bond results in the rehybridization of these carbon atoms and subsequent formation of a C–O bond of 143–145 pm in

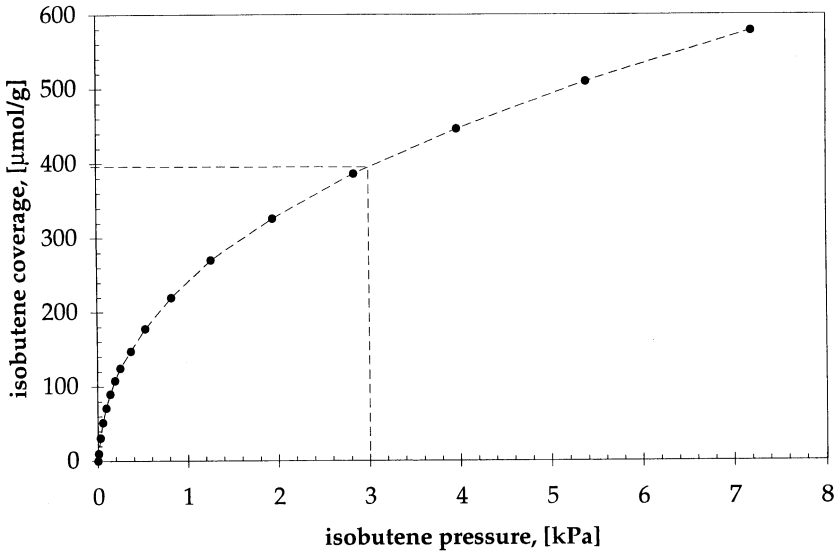

Figure 2. Adsorption isotherm for isobutene on silica at 300 K. The lines in the figure identify the point corresponding to the conditions at which the FTIR measurements were performed.

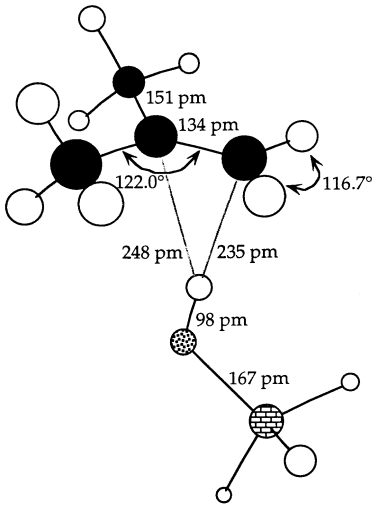

Figure 3. Structural model for molecularly-adsorbed isobutene on a (hydrogen-terminated) silanol group.

length. The length of the C–C bonds in the resulting alkoxy species is ~154 pm, which is the typical bond length for carbon atoms in a sp^3 state of hybridization. On the basis of the heats of reaction included in table 1, it appears that isobutoxy species are slightly more stable than 2-methyl-1-propoxy species by ~15 kJ/mol.

While the formation of butoxy species on silica seems to be favored thermodynamically, it is important to address the rate of formation of these species at room temperature. Accordingly, transition states corresponding to the reaction of molecularly-adsorbed isobutene to form the two possible alkoxy species were located on the PES. The optimized structures of these transition states are shown in figure 5, where TS1 and TS2 represent the complexes involved in the formation of 2-methyl-1-propoxy and isobutoxy species, respectively. As mentioned previously, it was verified that TS1 and TS2 are first-order saddle points (transition states) by ensuring that they have only one imaginary (negative) vibrational frequency. Furthermore, to verify that TS1 and TS2 are, in fact, the first-order saddle points that connect the desired reactant and products, IRC calculations were performed, the results of which are presented in figures 6 and 7. The structural models included in these figures correspond to the last point on each side of the IRC curves, and the models verify in both cases that the desired reaction products have been obtained.

In contrast to the structure of molecularly-adsorbed isobutene, the transition states show rehybridization of the carbon atoms previously engaged in the π-bond to a state between sp^2- and sp^3-hybridization. In addition, the O–H bond in the silanol group is stretched by 46 to 50 pm, and the carbon and oxygen atoms that bond in the corresponding alkoxy species are still too far from each other to be engaged in covalent interactions. The energetics of the elementary reactions leading to the formation of 2-methyl-1-propoxy and butoxy species from adsorbed isobutene are shown in table 1. The activation energies for the formation of these species from adsorbed isobutene are estimated to be 226 and 172 kJ/mol, respectively. These activation energies are higher than those estimated in previous studies of ethene adsorption on H-zeolites with high silica content [21–23], in which an activation energy of 64 kJ/mol was reported for the formation of ethoxy species from molecularly-adsorbed ethene. This difference is related to the acidity of the oxide under study, with H-zeolites being stronger acids than silica. On the basis of our DFT calculations, the formation of alkoxy species upon adsorption of isobutene on silica appears to be limited kinetically.

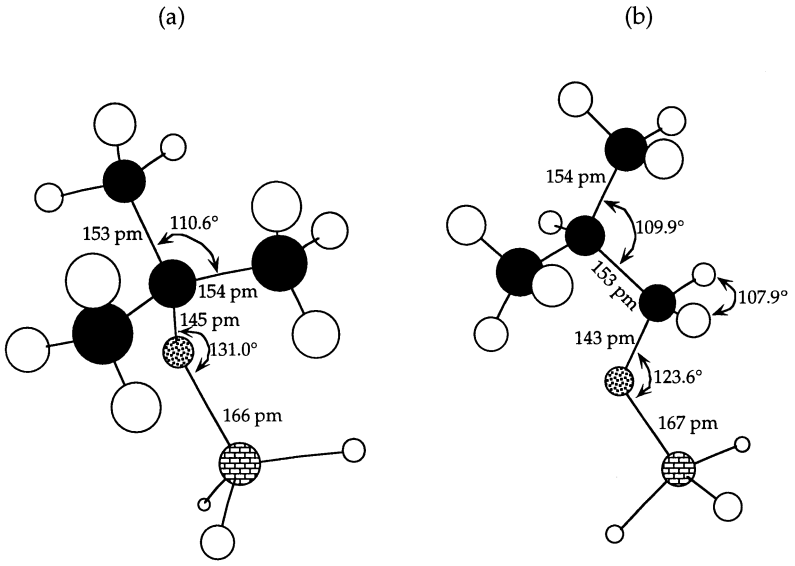

Figure 4. Structural models for (a) isobutoxy and (b) 2-methyl-1-propoxy species on a (hydrogen-terminated) silanol group.

Table 1
Energetics (kJ/mol) predicted for the adsorption and reaction of isobutene on a silanol group

Reaction at 298 K	ΔE	ΔH	ΔG	Accepted ΔH [a]
calibrations				
n-but-2-ene (trans) → isobutene	−2	−2	−1	−4
2-methyl-1-propanol → *t*-butanol	−25	−25	−23	−27
adsorption				
isobutene + H_3SiOH → isobutene(ads)- - -$HOSiH_3$	−7	−10	22	
protonation				
isobutene + H_3SiOH → isobutyl-$OSiH_3$	−52	−55	−3	
isobutene + H_3SiOH → 2-methyl-1-propyl-$OSiH_3$	−38	−40	10	
transition states				
reaction 1:				
isobutene(ads)- - -$HOSiH_3$ → TS1	226	226	237	
TS1→2-methyl-1-propyl-$OSiH_3$	−256	−256	−249	
reaction 2:				
isobutene(ads)- - -$HOSiH_3$ → TS2	172	172	183	
TS2 → isobutyl-$OSiH_3$	−217	−217	−207	

[a] Calculated using standard thermodynamic data.

This conclusion is examined further by analyzing IR spectra of isobutene on silica at room temperature presented in the next section.

The transition states involved in the formation of alkoxy species from adsorbed isobutene also form a pathway for the 1,2-hydride shift that converts isobutoxy to 2-methyl-1-propoxy species. Specifically, this 1,2-hydride shift is a two-step process, which takes place through the formation of adsorbed isobutene via transition states TS1 and TS2.

The high activation energies for the formation of butoxy species on silica can be interpreted in terms of the charge localized in the hydrocarbon fragment on the surface. The Mulliken charges of molecularly-adsorbed isobutene, isobutoxy, and 2-methyl-1-propoxy species on a silanol group are estimated to be equal to −0.04 *e*, −0.02 *e*, and +0.06 *e*, respectively. However, the Mulliken charges of the hydrocarbon fragment in transition states TS1 and TS2 are +0.47 *e* and +0.57 *e*, respectively. It is evident that the activation processes for the formation of isobutoxy and 2-methyl-1-propoxy species on silica involve the separation of charge, with the transition states resembling adsorbed carbenium ions. Since silica is a weak acid, the removal of a proton from a sila-

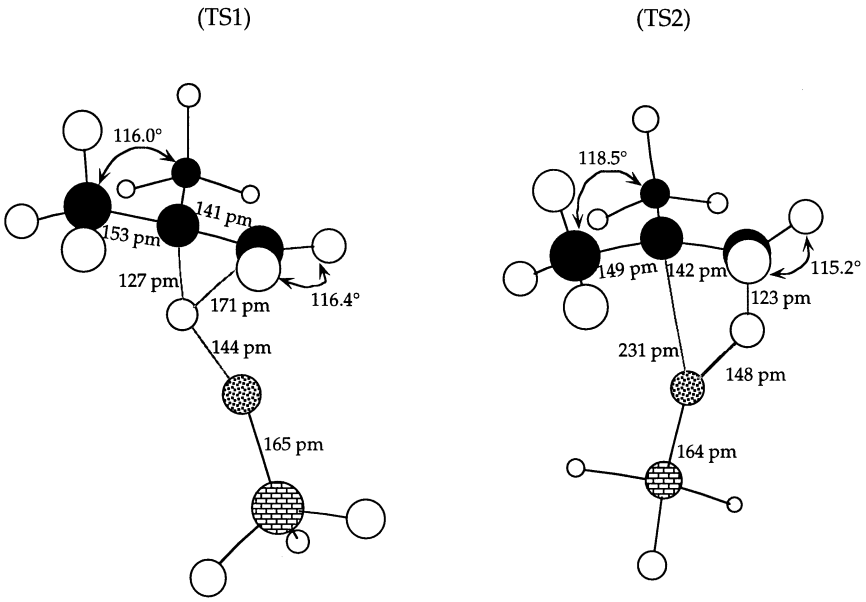

Figure 5. Structural models for the transition states involved in the formation of 2-methyl-1-propoxy (TS1) and isobutoxy (TS2) species on silica from molecularly-adsorbed isobutene.

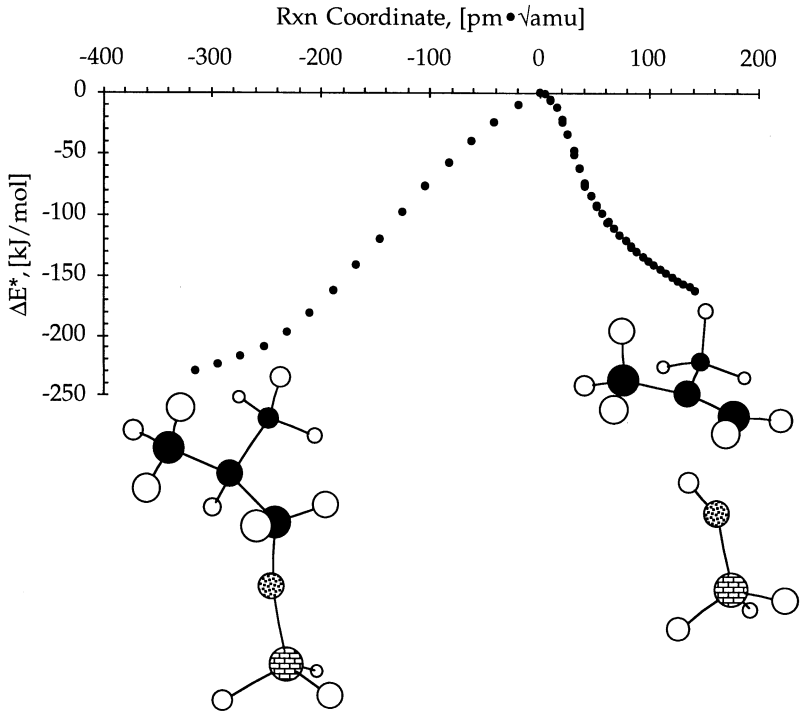

Figure 6. IRC calculation for the verification of TS1. Energies are defined relative to that of the transition state. The structural models in the figure correspond to the last point on each side of the curve.

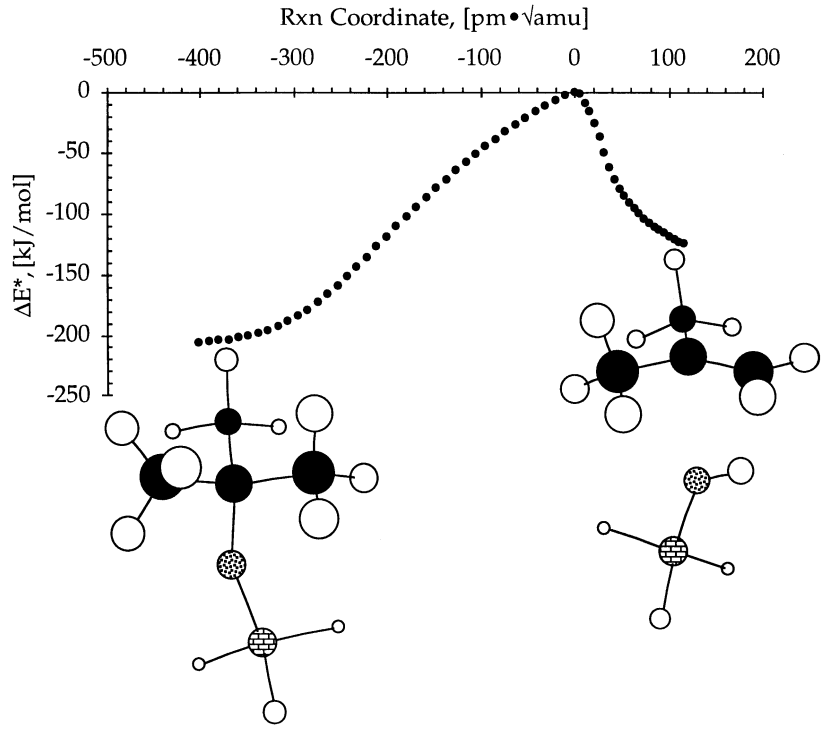

Figure 7. IRC calculation for the verification of TS2. Energies are defined relative to that of the transition state. The structural models in the figure correspond to the last point on each side of the curve.

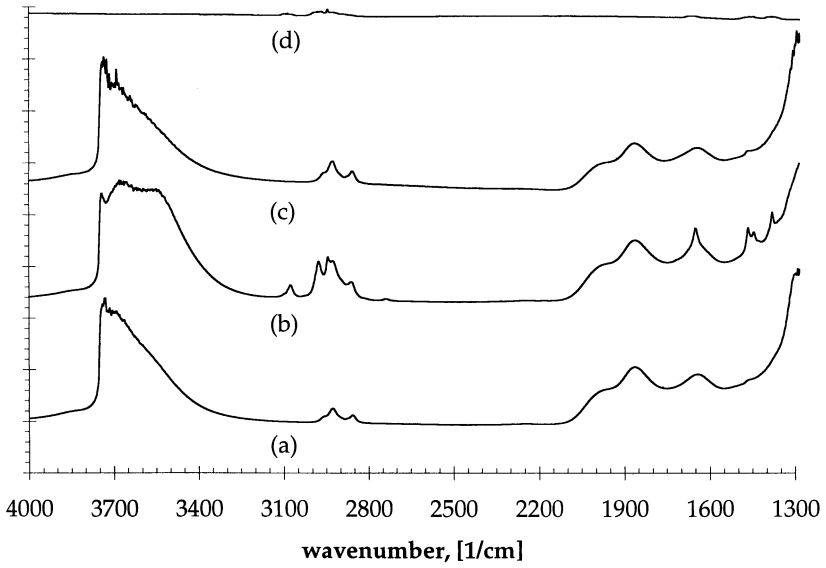

Figure 8. FTIR spectra of (a) silica, (b) isobutene adsorbed on silica at room temperature, (c) silica after exposure to isobutene, and (d) isobutene gas. The vertical scale is divided in 0.20 absorbance units.

nol group is a difficult step, thus leading to high activation barriers for the protonation of isobutene.

3.3. FTIR measurements

The IR absorption spectra for silica, gaseous isobutene, isobutene adsorbed on silica, and silica after exposure to isobutene are included in figure 8. The bands observed in the 2800–3000 cm^{-1} region of the spectrum corresponding to silica are due to absorption by minor amounts of hydrocarbon impurities, whose concentration may be reduced significantly by calcining the sample in oxygen at temperatures higher than 730 K. The spectra in figure 8 were subtracted from each other to generate difference spectra for isobutene adsorbed on silica and for silica after exposure to isobutene. These difference spectra are included in figure 9. The bands observed in the difference spectrum of isobutene on silica are summarized in table 2 and compared with the theoretical predictions from this work for adsorbed isobutene and literature data for gaseous isobutene. Most of the IR absorption bands appear to be unaffected by the adsorption process, except those corresponding to symmetrical and antisymmetrical stretches of C–H bonds in the CH_2

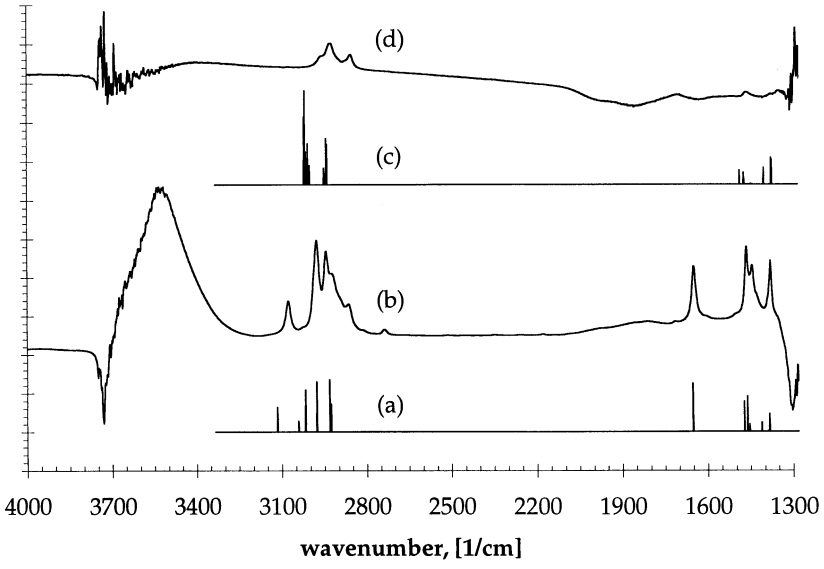

Figure 9. Difference FTIR spectra for (b) isobutene on silica and (d) silica after exposure to isobutene. The vertical scale is divided in 0.05 absorbance units. The spectra predicted by DFT calculations for (a) isobutene on silica and (c) isobutoxy species on silica have been included for comparison, with wavenumbers scaled by 0.966 so that the DFT calculations match the known IR bands for gaseous isobutene (see table 2).

Table 2
Wavenumbers (cm^{-1}) for isobutene in the gas phase (C_{2v} point group) and adsorbed on silica

Notation [a]	Symmetry	Description	Experimental [a]		DFT prediction [c]	
			gas [b]	adsorbed	gas	adsorbed
ν_{16}	B2	$\nu_{as}CH_2$	3087	3076	3116	3116
$\nu_4 + \nu_7$	B1		3019 (R)			
ν_1	A1	ν_sCH_2	2981	2978	3044	3041
ν_{11}, ν_{17}	A2, B1	$\nu_{as}CH_3$	2972 (R)			
ν_{25}	A1	$\nu_{as}CH_3$	2946	2946	3012	3018
ν_2	B2	$\nu_{as}CH_3$	2941		2964	2978
ν_3	B1	$\nu_{as}CH_3$	2928	2924	2924	2932
ν_{18}	A2	$\nu_{as}CH_3$	2893		2919	2927
$2\nu_{26}$	A1		2866	2864		
$2\nu_6$	A1		2817			
$2\nu_7$	A1		2747	2738		
$\nu_7 + \nu_9$	A1		2182			
$2\nu_{28}$	A1		1788			
ν_4	A1	$\nu C{=}C$	1660	1648	1666	1652
ν_5	A1	δ_dCH_3	1470	1464	1472	1472
ν_{19}	B1	ρ_tCH_3	1458		1460	1462
ν_{12}	A2	$\delta_{as}CH_3$	1459 (R)		1443	1442
ν_{26}	B2	$\delta_{as}CH_3$	1444	1444	1455	1454
ν_6	A1	δ_sCH_2	1430		1413	1412
ν_{20}	A1	δ_sCH_3	1386 (R)		1386	1388
ν_7	B2	δ_sCH_3	1381	1380	1384	1384
$\nu_{28} + \nu_{29}$	A1		1324			
ν_{21}	B2	$\nu_{as}C{-}C$	1281		1260	1264
ν_{27}	B1	ρ_wCH_3	1079		1078	1080
ν_8	A1	ρ_rCH_3	1062		1056	1058
ν_{23}	B2	ρ_rCH_2	980		957	918
ν_{28}	B1	ρ_wCH_2	888		885	886
ν_9	A1	$\nu_sC{-}C$	806		789	789

[a] (R): observed in Raman spectra.
[b] Taken from ref. [18] and references therein.
[c] DFT predictions have been scaled by 0.966 to obtain the best match between the theoretical and experimental spectra for gaseous isobutene.

group, an antisymmetrical stretch of C–H bonds in the CH_3 groups, the stretch of the C=C bond, and the stretch of surface hydroxyl groups. Specifically, shifts to lower wavenumbers of 11, 3, 4, and 12 cm^{-1} are observed for $\nu_{as}(CH_2)$, $\nu_s(CH_2)$, $\nu_{as}(CH_3)$, and $\nu(C{=}C)$, respectively. In addition, it is observed that C–H deformation modes and two of their overtones are shifted to lower wavenumbers by 1–9 cm^{-1}. For the stretching mode ν(O–H) of surface silanol groups, which is not included in table 2, a shift to lower wavenumbers of 212 cm^{-1}, from 3730 to 3518 cm^{-1}, is observed. Our DFT calculations predict a shift for ν(O–H) of 160 cm^{-1}, from 3819 to 3659 cm^{-1}. Our measured and calculated shifts of the $\nu(C{=}C)$ and ν(O–H) bands are in good agreement with previous investigations, in which shifts of 9–10 and 97–222 cm^{-1}, respectively, were observed [19,20]. These features are consistent with adsorptive interactions that mainly involve the π-bond in isobutene. The simultaneous perturbation of the ν(O–H) band corresponding to the surface silanol groups indicates that this interaction occurs through hydrogen bonding between these O–H groups and the π-bond in isobutene. The shifts to lower wavenumbers of the C–H stretching and deformation modes are consistent with the partial removal of electron density from the methyl and methylene groups as the π-bond interacts with surface silanol groups.

Even though most of the isobutene appears to adsorb reversibly on silica at room temperature, the difference spectrum for silica after exposure to isobutene suggests the accumulation of minor amounts hydrocarbon species. Broad bands with peaks centered at 2856, 2926, and 2964 cm^{-1} are observed. This experimental spectrum is compared in figure 9 with the IR spectrum predicted from DFT calculations for isobutoxy on silica. The good agreement between these spectra suggests that some butoxy species may form on silica and remain on the surface after evacuation of the sample at room temperature. Perhaps these species form on defect or impurity sites on the surface of silica.

The IR spectrum showing primarily adsorbed isobutene species was collected at an isobutene pressure of 3 kPa, and this pressure corresponds to a surface coverage of ~400 μmol/g. Since the average heat of isobutene interaction with silica for this surface coverage is 45 ± 4 kJ/mol (defined as the integral heat up to a coverage of 400 μmol/g divided by the total cov-

erage), we conclude that this heat corresponds to the formation of π-bonded isobutene species. For comparison, the corresponding heat of adsorption predicted from our DFT calculations was 10 kJ/mol, which is in agreement with experiment in view of the simplified model of the surface of silica used for our calculations.

The initial heat of isobutene interaction with silica is 56 kJ/mol. Since the IR spectrum collected after exposure and subsequent evacuation of isobutene from silica suggests the formation of small amounts of isobutoxy species, it is possible that the higher initial heats of adsorption are caused at least partially by the formation of these more strongly adsorbed alkoxy species. In this respect, the DFT calculations predict that isobutoxy species are more stable than π-bonded isobutene species by 45 kJ/mol.

4. Conclusions

(1) Isobutene primarily adsorbs reversibly on silanol groups on the surface of silica at 300 K. The average strength of the interactions between the π-bond and surface hydroxyl groups is 45 ± 4 kJ/mol at a coverage of $\sim$400 μmol of isobutene per gram of silica.

(2) The heats of formation of 2-methyl-1-propoxy and isobutoxy species from isobutene and silanol groups at 298 K are predicted to be 40 and 55 kJ/mol, respectively.

(3) The formation of alkoxy species upon reaction of isobutene with surface silanol groups appears to be limited kinetically, given that the activation energy is estimated to near 200 kJ/mol.

(4) The high activation barriers predicted for the formation of alkoxy species on silica are caused by the required localization of positive charge in the corresponding transition states, which is made difficult by the weak acidity of silica.

(5) Minor amounts of butoxy species may form on defect or impurity sites on silica.

Acknowledgement

The authors wish to acknowledge the financial support of the Office of Basic Energy Sciences of the Department of Energy, as well as the GEM and AOF fellowships awarded to MANS. The authors want to thank W.S. Millman for providing the IR cell used in our studies and K.B. Fogash for his interest and discussions during the course of the investigations.

Appendix

The structures of the molecular clusters presented in this report are defined in tables 3 and 4 in terms of cartesian coordinates to facilitate their visualization with any suitable software package.

Table 3
Optimized structures of clusters discussed in the text (coordinates listed in pm)

	Isobutene on silica			2-methyl-1-propoxy			Isobutoxy		
	x	*y*	*z*	*x*	*y*	*z*	*x*	*y*	*z*
C	−178.88	190.58	127.22	−188.98	85.51	−32.17	106.91	134.12	70.62
C	−119.19	237.96	−116.84	−17.14	268.28	7.28	183.78	−23.37	−110.90
C	−71.95	198.91	21.07	−41.54	126.01	−45.27	81.15	−0.06	0.55
C	57.30	173.52	47.75	50.52	27.36	27.03	83.51	−116.05	101.12
H	−255.87	117.37	99.36	−205.36	−16.01	−69.62	101.40	216.29	−1.62
H	−229.77	287.32	138.37	−253.44	153.83	−88.83	206.40	135.22	116.71
H	−137.90	161.97	224.59	−221.18	88.69	72.87	33.10	152.72	149.47
H	−36.80	242.22	−188.76	87.54	298.84	−5.02	163.54	−118.02	−162.23
H	−167.93	336.40	−114.47	−42.13	275.99	113.98	285.44	−26.73	−70.10
H	−193.86	166.58	−154.15	−79.53	340.69	−46.40	178.40	57.35	−184.73
H	90.84	147.45	147.93	24.78	24.09	134.19	182.68	−124.99	146.98
H	134.08	181.79	−28.92	155.08	60.71	18.43	60.06	−210.85	51.45
H	−18.10	−41.26	−12.40	−14.07	122.91	−151.73	10.98	−100.67	182.00
Si	72.35	−251.80	−31.25	122.53	−235.89	22.98	−201.89	0.54	−6.60
O	−43.79	−132.20	−36.34	37.05	−103.06	−29.77	−46.98	5.75	−66.46
H	185.44	−223.68	−124.21	269.36	−214.26	8.71	−236.93	−133.47	48.23
H	129.39	−268.34	105.48	94.17	−264.37	166.55	−224.66	100.67	101.51
H	4.36	−376.89	−72.16	79.03	−349.51	−61.40	−298.87	31.04	−121.85

Table 4
Optimized structures of transition states for the protonation of molecularly-adsorbed isobutene on silica to 2-methyl-1-propoxy (TS1) or isobutoxy (TS2) species (coordinates listed in pm)

	TS1			TS2		
	x	*y*	*z*	*x*	*y*	*z*
C	−227.72	−105.71	89.22	−143.68	−72.39	178.84
C	−228.42	26.84	−133.11	−226.09	4.16	−51.57
C	−158.12	−4.37	−1.26	−152.41	33.99	74.64
C	−76.59	94.40	57.35	−106.54	165.75	102.04
H	−244.56	−200.02	36.06	−128.71	−171.37	135.11
H	−325.75	−68.40	121.80	−239.52	−73.45	233.44
H	−168.04	−127.72	178.39	−64.12	−51.64	250.74
H	−169.19	94.94	−195.19	−201.16	75.50	−130.43
H	−326.47	73.03	−115.33	−333.91	13.35	−30.15
H	−245.32	−64.83	−190.70	−207.34	−97.55	−86.77
H	−46.20	88.96	161.34	−88.37	191.37	206.48
H	−46.75	183.39	2.98	−147.40	246.35	40.97
H	−42.48	−49.11	−28.30	0.80	132.71	52.66
Si	259.55	−30.48	−20.12	183.29	−66.80	−85.23
O	95.61	−13.70	−7.48	62.39	13.10	−8.89
H	306.24	−31.79	−162.23	228.41	0.02	−211.61
H	328.57	83.35	48.06	306.12	−84.25	−1.09
H	309.23	−156.64	43.04	138.44	−204.80	−123.89

References

[1] A. Corma, Chem. Rev. 95 (1995) 559.
[2] D. Seddon, Catal. Today 15 (1992) 1.
[3] G.M. Kramer, G.B. McVicker and J.J. Zieman, J. Catal. 92 (1985) 355.
[4] G.M. Kramer and G.B. McVicker, Acc. Chem. Res. 19 (1986) 78.
[5] N. Cardona-Martínez and J.A. Dumesic, J. Catal. 125 (1990) 427.
[6] S.A. Goddard, M.D. Amiridis, J.E. Rekoske, N. Cardona-Martínez and J.A. Dumesic, J. Catal. 117 (1989) 155.
[7] A.D. Becke, J. Chem. Phys. 98 (1993) 5648.
[8] W.J. Hehre, L. Radom and P von R. Schleyer, *Ab Initio Molecular Orbital Theory* (Wiley, New York, 1986) ch. 4.
[9] T. Ziegler, Chem. Rev. 91 (1991) 651.
[10] W. Kohn, A.D. Becke and R.G. Parr, J. Phys. Chem. 100 (1996) 12974.
[11] GAUSSIAN 94 (Revision C.2) , M.J. Frisch, G.W. Trucks, H.B. Schlegel, P.M.W. Gill, B.G. Johnson, M.A. Robb, J.R. Cheeseman, T. Keith, G.A. Petersson, J.A. Montgomery, K. Raghavachari, M.A. Al-Laham, V.G. Zakrzewski, J.V. Ortiz, J.B. Foresman, J. Cioslowski, B.B. Stefanov, A. Nanayakkara, M. Challacombe, C.Y. Peng, P.Y. Ayala, W. Chen, M.W. Wong, J.L. Andres, E.S. Replogle, R. Gomperts, R.L. Martin, D.J. Fox, J.S. Binkley, D.J. Defrees, J. Baker, J.P. Stewart, M. Head-Gordon, C. Gonzalez and J.A.J.A. Pople (Gaussian Inc., Pittsburgh, 1995).
[12] C. Peng, P.Y. Ayala, H.B. Schlegel and M.J. Frisch, J. Comp. Chem. 17 (1996) 49.
[13] C. Peng and H.B. Schlegel, Israel J. Chem. 33 (1993) 449.
[14] W.J. Hehre, L. Radom, and P. von R. Schleyer, *Ab Initio Molecular Orbital Theory* (Wiley, New York, 1986) ch. 7.
[15] C. González and H.B. Schlegel, J. Chem. Phys. 90 (1989) 2154.
[16] C. González and H.B. Schlegel, J. Phys. Chem. 94 (1990) 5523.
[17] I.N. Levine, *Quantum Chemistry* (Prentice Hall, Englewood Cliffs, 1991) p. 540.
[18] E. Valencia and A. Maldonado, J. Chem. Soc. Faraday Trans. 86 (1990) 539.
[19] G. Busca, G. Porcile and V. Lorenzelli, J. Mol. Struct. 141 (1986) 395.
[20] G. Busca, G. Ramis and V. Lorenzelli, J. Chem. Soc. Faraday Trans. I 85 (1989) 137.
[21] V.B. Kazansky and I.N. Senchenya, J. Catal. 119 (1989) 108.
[22] V.B. Kazansky, Acc. Chem. Res. 24 (1991) 379.
[23] I.N. Senchenya and V.B. Kazansky, Catal. Lett. 8 (1991) 317.